Molecular frame photoelectron angular distributions for core ionization of ethane, carbon tetrafluoride and 1,1-difluoroethylene

2016 J. Phys. B: At. Mol. Opt. Phys. 49 055203

(http://iopscience.iop.org/0953-4075/49/5/055203)

IOP Publishing Journal of Physics B: Atomic, Molecular and Optical Physics
J. Phys. B: At. Mol. Opt. Phys. **49** (2016) 055203 (11pp) doi:10.1088/0953-4075/49/5/055203

Molecular frame photoelectron angular distributions for core ionization of ethane, carbon tetrafluoride and 1,1-difluoroethylene

A Menssen[1,3], C S Trevisan[2], M S Schöffler[1], T Jahnke[1], I Bocharova[3], F Sturm[3], N Gehrken[1], B Gaire[3], H Gassert[1], S Zeller[1], J Voigtsberger[1], A Kuhlins[1], F Trinter[1], A Gatton[4], J Sartor[4], D Reedy[4], C Nook[4], B Berry[5], M Zohrabi[5], A Kalinin[1], I Ben-Itzhak[5], A Belkacem[3], R Dörner[1], T Weber[3], A L Landers[4], T N Rescigno[3], C W McCurdy[3,6] and J B Williams[1]

[1] Institut für Kernphysik, J. W. Goethe Universität, Max-von-Laue-Str. 1, D-60438 Frankfurt, Germany
[2] Department of Sciences and Mathematics, California State University, Maritime Academy, Vallejo, CA 94590, USA
[3] Lawrence Berkeley National Laboratory, Chemical Sciences, Berkeley, CA 94720, USA
[4] Department of Physics, Auburn University, Auburn, AL 36849, USA
[5] J R McDonald Laboratory, Kansas State University, Manhattan, KS 66506, USA
[6] Department of Chemistry, University of California, Davis, CA 95616, USA

Received 12 August 2015, revised 29 September 2015
Accepted for publication 20 October 2015
Published 15 February 2016

Abstract

Molecular frame photoelectron angular distributions (MFPADs) are measured in electron–ion momentum imaging experiments and compared with complex Kohn variational calculations for carbon K-shell ionization of carbon tetrafluoride (CF_4), ethane (C_2H_6) and 1,1-difluoroethylene ($C_2H_2F_2$). While in ethane the polarization averaged MFPADs show a tendency at low energies for the photoelectron to be emitted in the directions of the bonds, the opposite effect is seen in CF_4. A combination of these behaviors is seen in difluoroethylene where ionization from the two carbons can be distinguished experimentally because of their different K-shell ionization potentials. Excellent agreement is found between experiment and simple static-exchange or coupled two-channel theoretical calculations. However, simple electrostatics do not provide an adequate explanation of the suggestively simple angular distributions at low electron ejection energies.

Keywords: molecular photoionization, angular distribution, MFPAD

(Some figures may appear in colour only in the online journal)

1. Introduction

Time-dependent measurements of molecular frame photoelectron angular distributions (MFPADs) have been proposed as a method to probe the dynamics of unimolecular reactions in ultrafast experiments [1–4]. This idea is particularly promising because theoretical calculations of MFPADs suggest a strong sensitivity to molecular geometry [5, 6], but less sensitivity to the electronic state of the molecule [3, 4]. As a result of the development of new experimental techniques in recent years [7, 8], the angular distributions of photoelectrons viewed in the molecular frame are now being measured using several different methods, and it is generally recognized that they contain information about both the geometry of the molecule and the dynamics of photoejection.

For ejected electron energies below about 15–20 eV the shapes of MFPADs from core hole ionization frequently have simple forms that suggest that they may have a correspondingly simple physical origin. For example, measurements of the MFPADs at low energies for the methane molecule [9] reveal a dramatic apparent 'imaging' of the molecular geometry, in the sense that when averaged over polarization directions, both measured and calculated MFPADs showed a strong tendency for an electron ionized from the carbon 1s level to be ejected along the direction of the bonds in the molecule. Subsequent theoretical calculations demonstrated

that polarization averaged MFPADs show this 'imaging' effect in some cases [5] but not in others [3, 6]. In fact, the opposite behavior, which might be called 'anti-imaging', is also seen in calculations of MFPADs for some molecules in which the ejected core electron seems to be directed away from the directions of bonds in the molecule [6] in an energy-dependent effect that has been interpreted in terms of the chemical electronegativity of the atomic species involved.

Following core hole ionization, Auger decay generally ejects one or more additional electrons, leading to the dissociation of the resulting molecular dication (or trication if double Auger decay occurs). By measuring the momenta of the resulting ionic fragments and the photoelectron in coincidence, experiments using the COLd target recoil ion momentum spectroscopy (COLTRIMS) technique[10, 11] can measure either MFPADs or recoil frame photoelectron angular distributions (RFPADs), in which the MFPAD is effectively averaged around the axis of recoil of a pair of ionic fragments. In channels in which the orientation of the recoiling fragments would be required to establish the orientation of the molecular frame, only RFPADs can be measured. For polyatomic molecules, these measurements, especially when combined with theoretical calculations of the angular distributions, can reveal the mechanisms and dynamics of dissociation of the resulting molecular cations [7, 12, 13].

Here we explore the physics of low energy MFPADs with experimental determinations of MFPADs and RFPADs for three molecules, carbon tetrafluoride (CF_4), ethane (C_2H_6) and 1,1-difluoroethylene ($C_2H_2F_2$), combined with *ab initio* complex Kohn variational calculations of the differential cross sections for K-shell photoejection. The first of these molecules was previously predicted to show the opposite of the 'imaging' effect [6, 14] at low ejection energies. The case of ethane is analogous to methane, and falls into the class of molecules with hydrogen atoms bonded to heavier atoms which were speculated to be candidates to produce 'imaging' MFPADs with a tendency for core electrons to be ejected along those bonds at low energies [5]. Difluoroethylene is a case which combines both kinds of bonds, those between hydrogen and a heavier atom and those between second row atoms, and thus might be expected to combine these effects.

It is worth noting at the outset that, as seen in both experimental measurements and theoretical calculations, the MFPAD for a fixed direction of the polarization axis relative to the molecule is almost always dominated by the tendency of the ionized core electron to be ejected primarily along the polarization axis, with some modifications of the expected dipole pattern by scattering from the ion and applicable selection rules. That usually dominant physical effect is masked by averaging over the directions of the polarization axis, and would be extinguished altogether if there were only a $\cos^2\theta$ dipole dependence on the angle between the ejected electron and the polarization axis. It is what remains that constitutes the polarization averaged MFPAD, whose frequently simple shape has been the subject of the recent literature. Both polarization-fixed and polarization-averaged MFPADs contain more detailed information about the interaction of the ejected electron with the residual ion than there is in the photoionization of a randomly oriented ensemble of molecules that produces the familiar $1 + \beta(E)\,P_2(\cos(\theta))$ angular distribution, where P_2 is a Legendre polynomial and $\beta(E)$ is the asymmetry parameter.

The outline of this paper is as follows. In the following section we briefly describe the experimental methods used in these measurements. Section 3 describes the theory of MFPADs and summarizes the complex Kohn variational method used in the calculations we present. Results and comparisons between experiment and theory for the three molecules we consider here are presented in section 4. We conclude with some ideas on the origins of the shapes of low energy MFPADs in section 5.

2. COLTRIMS measurement of MFPADs

The experiment was performed at beamline 11.0.2.1 at the advanced light source at the Lawrence Berkeley National Laboratory (LBNL). The COLTRIMS method [10, 11] was employed to measure the momenta of the charged fragments created in the photoreaction. In brief, the 3D-momenta of the photoelectrons and ions created by ionizing the molecular target are measured in coincidence by guiding these particles onto two time- and position-sensitive detectors employing homogenous electric and magnetic fields. By reconstructing the trajectory of each charged particle inside the spectrometer, its momentum vector is obtained. The trajectories are deduced from the position of impact on the detector, the time-of-flight of each particle, and the knowledge of the spectrometer geometry, the applied fields and the location of the interaction region inside the spectrometer. The latter is created by crossing a supersonic gas jet (consisting of the species to be investigated) with the photon beam from the synchrotron at right angles.

The ion arm of the COLTRIMS analyzer consisted of a single acceleration region with a length of 3.65 cm. The electron arm employed a McLaren time-focussing scheme consisting of an accelerating region of 7.2 cm and a drift region of 13.8 cm. The recoiling ions and electrons experience the same electric field of approximately 12 V cm^{-1}. In order to observe the electrons of interest with full solid detection angle a magnetic field of 4.2 Gauss parallel to the momentum spectrometer time-of-flight axis was employed.

The momenta of the ejected photoelectron and ionic fragments produced by Auger decay and subsequent dissociation of the resulting dication or trication (if double Auger decay is possible) are measured in the laboratory frame. In order to obtain photoelectron angular distributions in the molecular frame from the measured data, the molecular frame must be determined from coincidence measurements of the momenta of ionic fragments and the ejected electron. For the case of CF_4, for example, the determination of the molecular frame is illustrated in figure 1 which shows the momenta of F^+ ions measured in coincidence. The momenta of two recoiling F^+ ions span a plane. If the magnitudes of their momenta are the same, the sum of the two measured F^+ ions

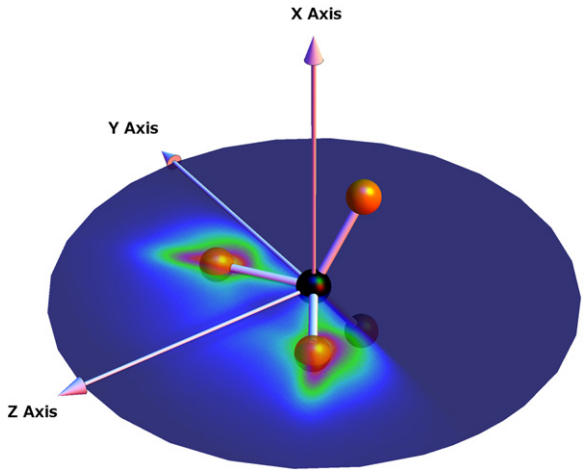

Figure 1. Distribution of momenta of the F^+ ions measured in coincidence from the dissociation of CF_4 after core hole ionization followed by Auger decay, plotted in the FCF molecular plane.

defines the z-axis (C_2 symmetry axis) of the FCF plane of the molecule. The assumption of equal momenta for the F^+ ions is verified as seen in the momenta plotted in figure 1 from the COLTRIMS coincidence measurements. The determination of the orientation of the FCF plane is sufficient to determine the absolute orientation of this molecule because of its tetrahedral symmetry. This analysis assumes that the conditions of the 'axial recoil' approximation holds, in which the dissociation is prompt and direct, occurring in much less time than any rotation or rearrangement dynamics in the ion. The orientation of difluoroethylene is determined similarly from the channel producing two H^+ ions.

Our experimental determination of MFPADs assumes that the target molecules have only zero point motion about their equilibrium geometries. Because of cooling through the expansion of the gas jet, target molecules are expected to have internal temperatures in general less than 80 K and in the case of ethane of about 30 K [15]. Of the cases studied here the molecule with the lowest energy vibrational mode is ethane, whose a_{1g} torsional mode has an excitation energy 289 cm^{-1} [16]. At its temperature in the gas jet the ground state population of even this vibrational mode has a population of over 99.4% (at 80 K).

The MFPAD shapes at low energies that we focus on below are the results of averaging over all polarization directions in the molecular frame, which is accomplished by accumulating data in the molecular frame for all orientations of the molecular frame relative to the laboratory frame polarization axis.

3. Calculations of MFPADs using the complex Kohn variational method

MFPADs for photoionization are determined from matrix elements of the dipole operator between the initial neutral electronic state of the molecule and the electron–ion scattering wave function for an electron scattering from the cationic state of the molecule that is produced. In the case of K-shell ionization in molecules with first row atoms, we have found that a single determinant initial state wave function for both the neutral target and final cation state is generally sufficient to produce integral and differential cross sections that agree reliably with experiment for ejected electron energies from a few eV up to few tens of eV [5, 9]. In particular the shapes of the MFPADs are well described by this simple approximation. Depending on the system, such results can be obtained with the single determinant cation wave function constructed with either orbitals from a self-consistent field calculation on the neutral or the cation, and as a refinement we can use natural orbitals from the averaged density matrices of the ion and neutral molecules, effectively applying what is known as 'Slater's transition state approximation' [17] for the photoionization process. For the calculations reported here, orbitals from a Hartree–Fock calculation on the neutral molecule were used in all cases.

To produce the electron–ion scattering wave function we used the complex Kohn variational method for electron-molecule scattering, with modifications needed to treat electron scattering from molecular ions [18]. Details about how the complex Kohn method is applied to molecular photoionization have been given previously [3, 5, 19, 20] and will not be repeated here. In the case of CF_4, where there is a single carbon atom, we can use single-channel static-exchange calculations for the electron–ion scattering wave function. This is also the case for 1,1 difluoroethylene, where the molecular orbitals corresponding to the carbon bonded to two hydrogens or the carbon bonded to two fluorines have Hartree–Fock orbital energies that differ by 5.2 eV (experimental splitting is 4.8 eV [21, 22]). In the case of ethane, however, where there are two nearly degenerate ion states that arise from the removal of an electron from the $1a_{1g}$ or $1a_{1u}$ orbitals in the ground state configuration $1a_{1g}^2 1a_{1u}^2 2a_{1g}^2 1a_{2u}^2 1e_u^4 3a_{1g}^2 1e_g^4$, those two ionization channels must be treated in a two-state close-coupling complex Kohn calculation. In such cases, separate one-channel channel calculations fail even to produce MFPADs that when averaged over the direction of polarization reflect the inherent symmetry of the molecule, which is an essential characteristic of the physical result. The Kohn variational trial functions in these calculations were built from Gaussians and single-center numerical continuum functions with angular momenta up to $\ell = 6$ for CF_4 and difluoroethylene, and up to $\ell = 4$ for ethane. CF_4 and difluoroethylene require more angular functions for convergence than ethane because of the presence of heavy atoms off the center of mass in the first two cases.

The MFPAD for a fixed direction of the polarization vector is related to the dipole matrix element between the neutral and electron–ion scattering wave functions via the relation

$$\frac{d^2\sigma^{\Gamma_0}}{d\Omega_{\hat{k}} d\Omega_{\hat{\epsilon}}} = \frac{8\pi\omega}{3c} \left| \hat{\epsilon} \cdot \langle \Psi_0 | \hat{\mu} \left| \Psi^-_{\Gamma_0, \vec{k}_{\Gamma_0}} \right\rangle \right|^2 \qquad (1)$$

which defines the cross section for polarization $\hat{\epsilon}$ and ejected electron momentum $\vec{k}_{\Gamma_0}$ leaving the ion in state Γ_0. The complex Kohn scattering calculation produces the final state wave function $\Psi^-_{\Gamma_0,\vec{k}_{\Gamma_0}}$ in this expression. In this study we present MFPADs for fixed polarization direction as well as integrated over all polarizations, in both cases with the molecule in a fixed orientation. It is the polarization-averaged MFPAD that is seen in some cases to appear to 'image' the molecule.

There is a key difference between the information contained in the measurements with $\hat{\epsilon}$ fixed or averaged over its orientations. In computing the differential cross section for fixed polarization via equation (1), the matrix elements of the three cartesian components of the dipole operator are added coherently. In terms of those cartesian components, we can write

$$I_{\vec{k}_{\Gamma_0}\hat{\epsilon}} = \hat{\epsilon} \cdot \langle \Psi_0 | \hat{\mu} \left| \Psi^-_{\Gamma_0,\vec{k}_{\Gamma_0}} \right\rangle = \hat{\epsilon} \cdot \vec{M}_{\vec{k}_{\Gamma_0}}. \quad (2)$$

Integration over the directions of $\hat{\epsilon}$ then gives

$$\int \frac{\mathrm{d}^2\sigma^{\Gamma_0}}{\mathrm{d}\Omega_{\hat{k}} d\Omega_{\hat{\epsilon}}} d\Omega_{\hat{\epsilon}} = \frac{8\pi\omega}{3c}\frac{4\pi}{3}\left(\left| M^x_{\vec{k}_{\Gamma_0}} \right|^2 + \left| M^y_{\vec{k}_{\Gamma_0}} \right|^2 + \left| M^z_{\vec{k}_{\Gamma_0}} \right|^2 \right). \quad (3)$$

While the coherent combination of the transition dipole amplitudes can produce a wide variety of shapes of the MFPAD for different polarization directions, the experiment that measures the MFPAD averaged over polarization directions measures an incoherent sum of the same three amplitudes.

We also calculated MFPADs averaged around the C–C bond axis in the case of ethane but with the polarization vector fixed at particular angles to that axis to compare with the measured recoil frame photoelectron angular distributions (RFPADs). These averages were accomplished by choosing a grid of electron directions $\hat{k}$ for different orientations of the molecule with respect to photon polarization, performing separate calculations of the MFPAD for each orientation and using Shepard interpolation [23] to evaluate the average. Those results will be used in section 4 for comparison with RFPADs measured in the $[CH_3^+, CH_3^+]$ dissociation channel.

4. Results

The three molecules we are reporting results for in this study were chosen because their carbon K-shell photoelectron angular distributions all reveal aspects of the underlying molecular geometry, but in strikingly different ways.

4.1. Ethane

Results for ethane are presented in figures 2–4 for a photon energy of 298 eV and linear polarization of the incoming light. Since the carbons in this molecule are bonded to hydrogens, ethane falls into the class of molecules for which 'imaging' at low energies might be expected from earlier theoretical and experimental studies. The predicted result in the right column of figure 2 shows the same imaging effect we calculated and measured previously for methane in the polarization-averaged MFPAD.

Among the breakup channels that are observed, the one that produces three protons following double Auger decay has the potential to allow complete determination of the molecular frame

$$C_2H_6 + h\nu \rightarrow C_2H_6^+\left(C\ 1s^{-1}\right) + e^- \rightarrow H^+ + H^+ + H^+ + \text{neutrals} + 3e^-. \quad (4)$$

In this channel we observe that the protons emerge with mutual angles between their momentum vectors of approximately 100° and with equal magnitudes. That result is shown in figure 2, which was produced by applying gates to the data that select events in which the angles between the proton momentum vectors are greater than 60° and less than 140°. Newton plots, similar to the ones made in our earlier work [9, 13], were used to determine the choice of these gates. It should be noted that the clean compact islands in the Newton plots with equal angles between the proton momenta strongly suggest that this was a prompt dissociation and allow us to discard the possibility of a sequential dissociation process. All of the experimental MFPADs have been smoothed by averaging each bin with all of the adjacent bins.

In the absence of detailed information about the dynamics of dissociation in this channel it is reasonable to begin the analysis of the data with the assumption that the protons emerge near the directions of the bonds, as they do in a similar double Auger breakup channel in the case of methane [9, 13]. There are two cases that might be distinguished: (1) three protons emerging from one carbon or (2) two protons from one carbon and one proton from the other. The angles between the proton momenta that might be expected from recoil along the bonds are indicated in figure 3. The observed recoil angles do not exactly match the 108° angle (the observed angle is approximately 100°, as noted above) that would be expected from this simple picture of 'bond recoil' if the protons originate from one side of the molecule but no distinct feature is present in the data that would suggest the unequal angles between the proton momentum vectors shown in figure 3 for the case in which the protons originate from different ends of the molecules.

Figure 2 shows the experimental MFPAD that results from analyzing this data under the assumption that all three protons originate from the same side of the molecule. Although there is some indication of the six lobes of the MFPAD along the bond directions seen in the complex Kohn scattering calculations presented in the same figure, it is clear that the match between experiment and theory is poor. We speculate that, since we are not able to determine whether the protons originate from one side of the molecule or not in this experiment, the molecular frame has not been unambiguously determined. Performing the same experiment using deuterated ethane, CD_3CH_3, with all three deuterons on the same carbon would in principle allow complete determination of the molecular frame, and could also shed light on the possible

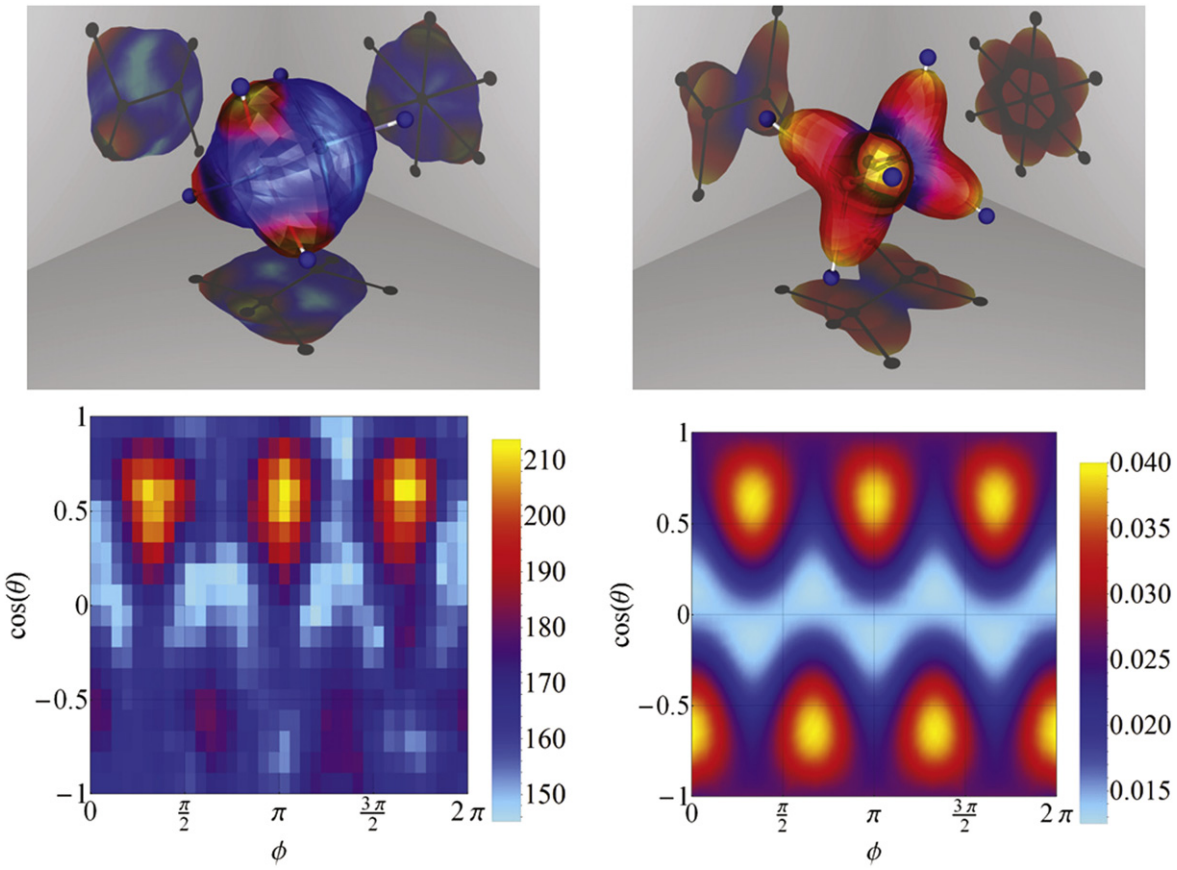

Figure 2. MFPAD for C_2H_6 at 4.5 eV above the C 1s threshold from analysis of the experimental data assuming the three protons in the breakup channel $C_2H_6 + h\nu \rightarrow H^+ + H^+ + H^+ + \text{neutrals} + 3e^-$ originated from the same carbon atom (left column) and complex Kohn calculations at 4.35 eV (right column).

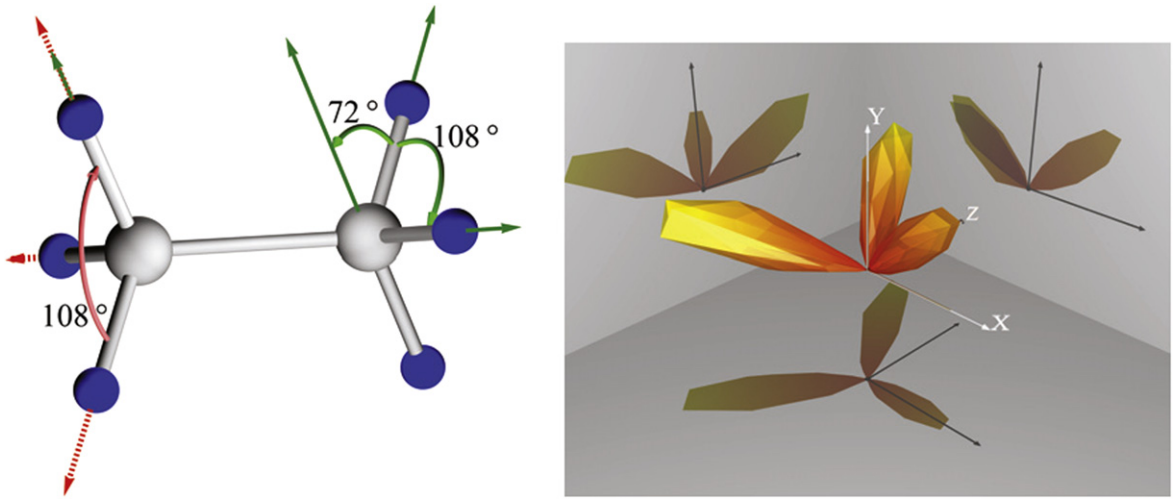

Figure 3. Left: approximate relative angles between the momenta of three emerging protons under the assumption of recoil along the directions of bonds. Dashed arrows indicate three protons from the same carbon, and solid arrows indicate two protons from one side and one from the other. Right: observed proton angular distribution that was used to produce the experimental MFPAD in figure 2.

breakdown of the axial recoil approximation in the dynamics of dissociation in this case.

However, strong experimental evidence that the theoretical prediction is correct and that the MFPAD does in fact have lobes along the bonds in ethane is provided by measurements of the RFPAD in the two-body symmetric breakup channel

$$\begin{aligned} C_2H_6 + h\nu &\rightarrow C_2H_6^+\left(C\ 1s^{-1}\right) + e^- \\ &\rightarrow CH_3^+ + CH_3^+ + 2e^-. \end{aligned} \tag{5}$$

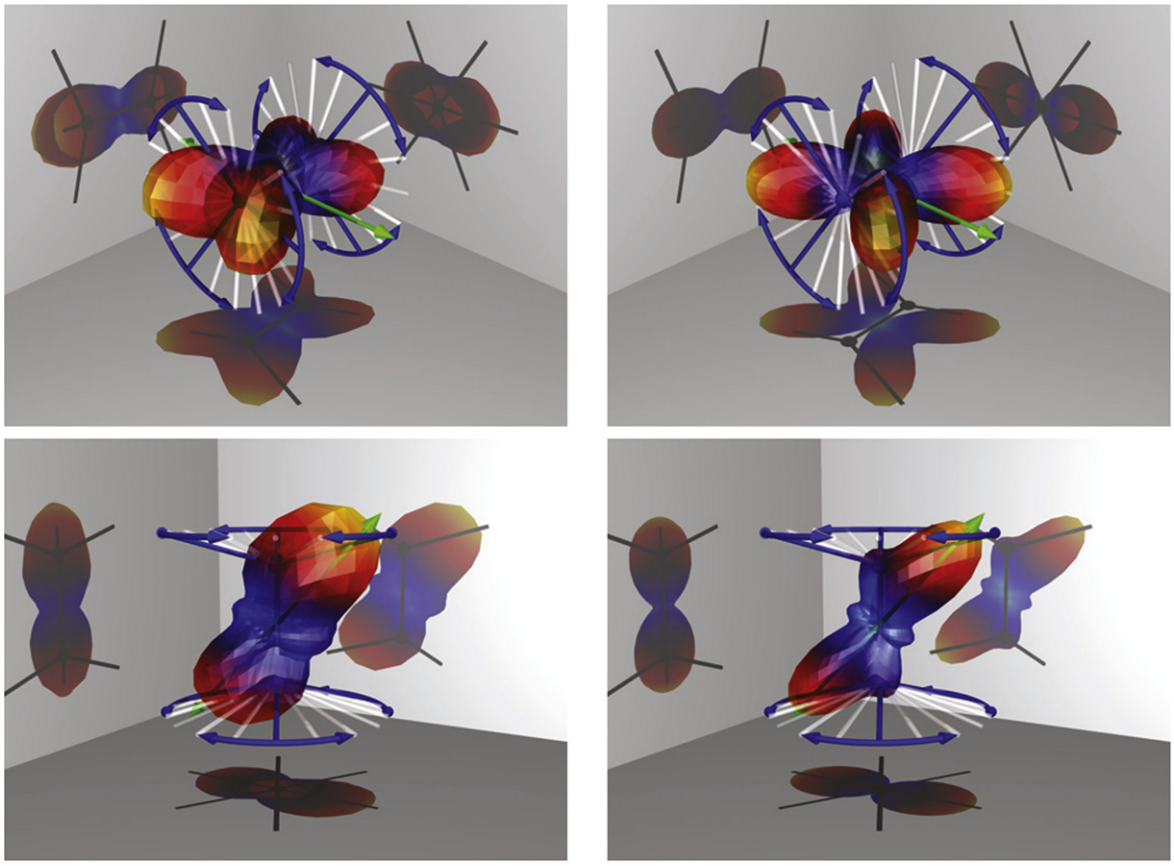

Figure 4. RFPADs for the $CH_3^+ + CH_3^+$ break up channel from experiment (left column) and complex Kohn calculations (right column) with polarization perpendicular to the C–C bond (top row) and at 45° to the C–C axis (lower row) as indicated by the straight double headed arrow. The curved arrows indicate the effective averaging around the C–C bond axis that occurs in this RFPAD measurement.

In this case the recoil axis accurately determines the molecular axis in the experiment. The comparison of theory and experiment for these RFPADs in figure 4, using precisely the same theoretically computed photoionization amplitudes that were averaged over polarizations to give the MFPAD in figure 2, shows nearly perfect agreement. That comparison substantially validates the theoretical prediction, and we conclude that the imaging effect is present at low photoejection energies in the case of ethane. In both configurations the tendency of the outgoing electron to follow the axis of polarization is evident, modified by scattering from the molecule. In the case with the polarization perpendicular to the C–C bond axis the four lobes originate from the imaging effect seen in the MFPAD, here averaged around the C–C axis and focused in the plane of that axis and the polarization axis. Note that with the polarization perpendicular to the C–C bond, theory (figure 4, top right) shows a nodal plane perpendicular to the axis of polarization, in which electron ejection vanishes. This behavior is due to a dipole selection rule originating from the symmetry of the molecule and the electronic state of the ion being produced. The fact that this plane is somewhat filled in figure 4, top left, is due to the finite range of acceptance angles for the electron and ions detected in the experiment.

4.2. Carbon tetrafluoride

Several fragmentation channels occur following photoionization of CF_4 less than 10 eV above the carbon K-edge threshold energy. A detailed study of the fragmentation processes following photoionization at these energies has been conducted in [24]. In the present experiment the following decay channels have been observed:

$$\begin{aligned} CF_4 + h\nu \rightarrow CF_4^+\left(C\ 1s^{-1}\right) + e^- &\rightarrow CF_4^{2+} + 2e^- \\ &\rightarrow F^+ + CF^+ + \text{neutrals} + 2e^- \\ &\rightarrow F^+ + F^+ + \text{neutrals} + 2e^- \\ &\rightarrow C^+ + F^+ + \text{neutrals} + 2e^-. \end{aligned} \quad (6)$$

In order to gather the photoelectron angular distributions in the molecular frame, the break-up channel consisting of two singly charged fluorine ions was examined. The measurements were performed at a photon energy of ∼306 eV. The threshold of the carbon K-edge of CF_4 is located at 301.8 eV [24, 25], so our experiments yield photoelectrons with a kinetic energy of ∼4 eV.

Figure 5 depicts the MFPAD of these electrons when averaged over the polarization direction. While the polarization-averaged MFPAD clearly reflects the symmetry of the

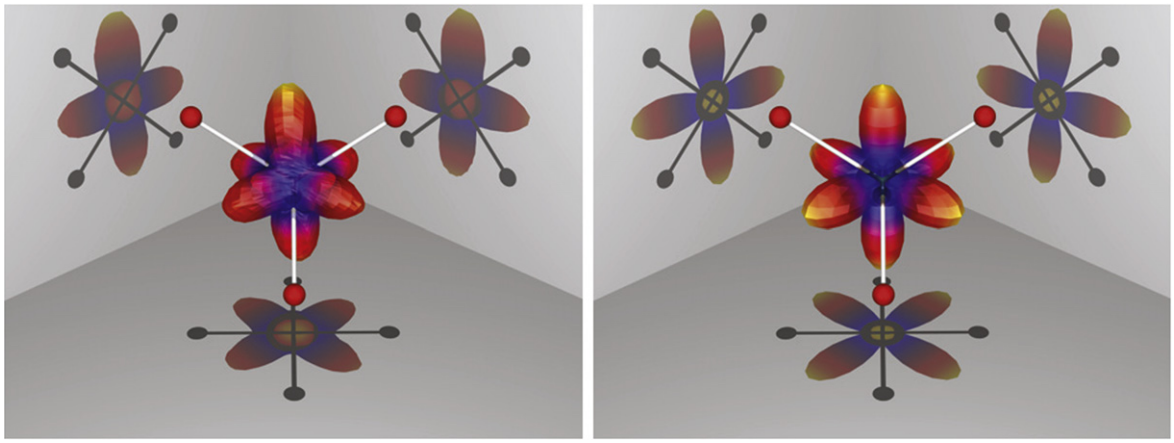

Figure 5. MFPAD for K-shell ionization of CF_4. Left: the observed photoelectron distribution measured in coincidence with $F^+ + F^+$ following Auger decay. Right: the MFPAD calculated using the complex Kohn variational method. Data and theory are integrated over all orientations of the polarization vector. The equilibrium molecular geometry is represented by the ball and stick models.

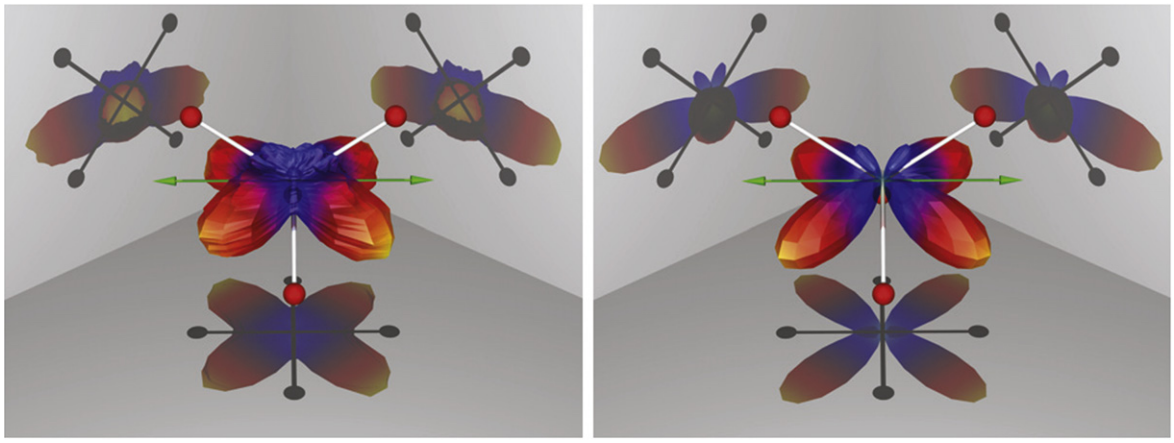

Figure 6. MFPAD for K-shell ionization of CF_4 with the polarization fixed perpendicular to the C_2 axis and in the plane of two C–F bonds. Left: the observed photoelectron distribution measured in coincidence with $F^+ + F^+$ following Auger decay. Right: the MFPAD calculated using the complex Kohn variational method. The equilibrium molecular geometry is represented by the ball and stick models and the polarization axis by the double headed arrow.

target molecule, the pattern of preferential photoelectron emission contrasts sharply with that found for ethane (and methane). In this case, the photoelectron emission peaks between the fluorines, in line with findings previously reported [6, 14] that suggest the opposite of the imaging effect in this molecule.

Additional detail for this case can be obtained by examining MFPADs for different orientations of the molecule with respect to the polarization vector of the ionizing light. Such a configuration is depicted in figure 6 where the polarization vector is chosen perpendicular to a C_2 axis and in the plane of two C–F bonds (FCF plane). The propensity for ejection away from the fluorine atoms is still present, but a dipole selection rule in this configuration arising from the molecular symmetry prevents photoelectron ejection in the plane perpendicular to the polarization axis and extinguishes the prominent vertical lobes found in figure 5. Even the minor lobes of the theoretical MFPAD are observed in the experiment in figure 6, verifying that the simple static-exchange description of core photoionization is sufficient for this case.

4.3. Difluoroethylene

Given the contrasting behavior we found in the MFPADs for C_2H_6 and CF_4, we examined 1,1-difluoroethylene ($C_2H_2F_2$) which might be expected to show properties of both the other molecules as it contains two carbon atoms, one bound to two fluorines, while the other is bound to two hydrogens. Moreover, the binding energy of K-shell electrons belonging to either carbon atom differs by almost 5 eV which allows the experiment to distinguish which carbon atom is being ionized, since photoelectrons coming from the fluorine side or the hydrogen side will differ in energy by ~5 eV.

In order to minimize differences due to different energies of the ejected photoelectrons, we performed two measurements at photon energies of $h\nu = 296$ and $h\nu = 301$ eV. The first measurement yielded photoelectrons near ~0 and 5 eV, while photoelectrons near 5 and 10 eV are created in the

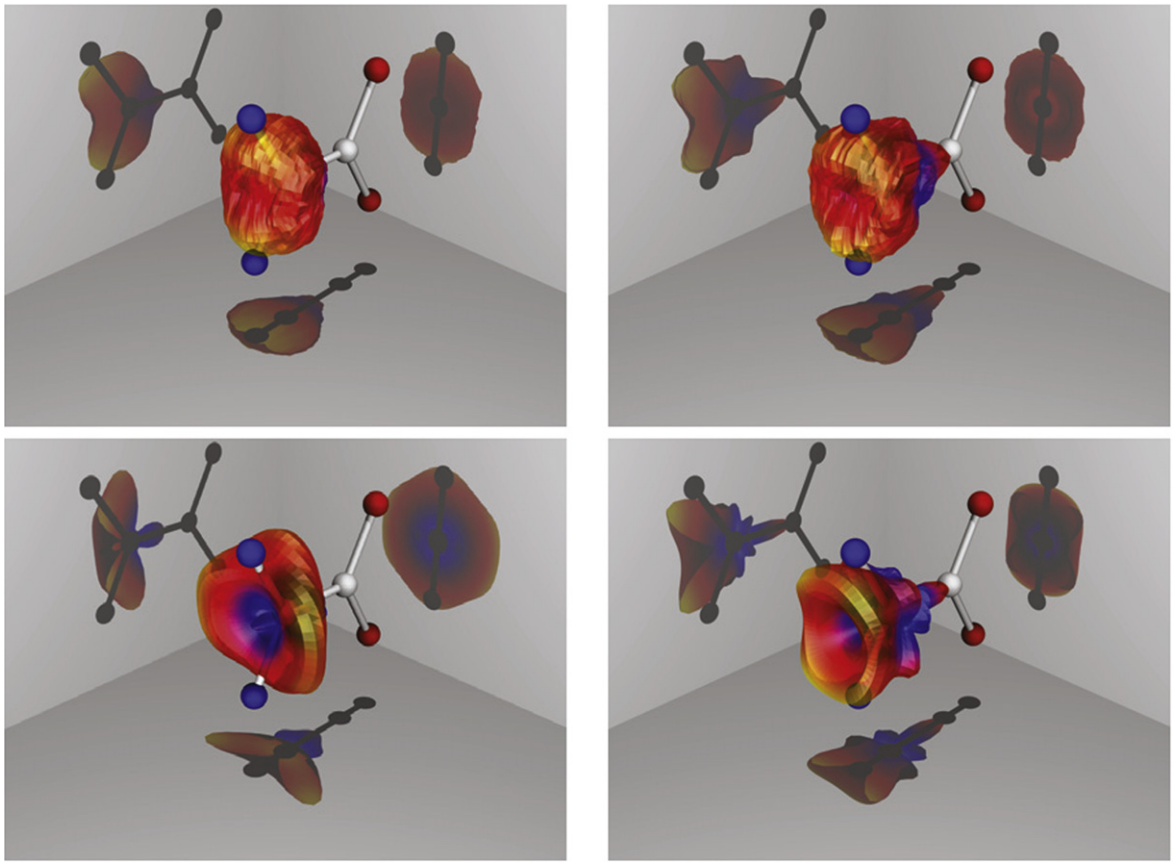

Figure 7. MFPADs of $C_2H_2F_2$ where the carbon on the H_2 side was ionized in experiments performed at two different photon energies: $h\nu = 296$ and $h\nu = 301$ eV. Top row: experiment 4–6 eV and 8–12 eV photoelectrons. Bottom row: complex Kohn results at photoelectron energies of 5.44 and 10.88 eV.

second measurement [21, 22]. In that way data sets were created for photoelectrons of a kinetic energy of 5 eV after emission from either carbon atom.

The ground state geometry of $C_2H_2F_2$ is planar [26]. In order to establish the orientation of the molecule in the laboratory frame we investigated fragmentation channels producing two protons

$$\begin{aligned} C_2H_2F_2 + h\nu &\rightarrow C_2H_2F_2^+\left(C\ 1s^{-1}\right) + e^- \\ &\rightarrow H^+ + H^+ + \text{neutrals} + 2e^-, \end{aligned} \tag{7}$$

where the photoionization step produces a K-shell vacancy in one or the other of the carbons. Because the molecule is planar, the detection of two protons, under the assumption of axial recoil, suffices to provide the absolute orientation of the molecule in the laboratory frame.

Figure 7 shows the MFPAD at two energies resulting from carbon 1s photoejection on the side bonded to hydrogen. Theory and experiment both show that there is a strong propensity for photoemission directed away from the fluorine side of the molecule, as expected. The corresponding MFPADs for photoejection from the fluorine side of the molecule are shown in figure 8. We again see a propensity for photoelectrons to avoid the fluorine atoms, but in this case the effect is more subtle. There is photoejection on the fluorine side of the molecule, but it is directed preferentially in the plane perpendicular to the FCF plane.

The agreement between theoretical predictions of the MFPADs and the experimental observations in the case of difluoroethylene is in general satisfactory, but not as good as in the other cases studied here, particularly in the example in figure 8 in which photoelectrons with energies between 0 and 2 eV are produced. Although the experimental angular resolution is poorer for electrons with near zero kinetic energy, and there is also the possibility of post collision interaction in which low energy photoelectrons are influenced by subsequent Auger decay [27], neither of these effects can completely explain the descrepancy between theory and experiment at these energies. Given the success of the static-exchange approximation in the other cases studied here which involve the same atoms, as well in other comparisons with MFPADs measured in similar COLTRIMS experiments [7, 9, 13], there is no obvious reason to suspect that either the theoretical treatment or the experimental techniques should be intrinsically less accurate in this case. Both in this case, and in the case of the dissociation channel in the ethane data that produces three protons, the discrepancies between experiment and theory may thus call into doubt the assumption that the axial recoil approximation is an adequate description of the dissociation dynamics following Auger decay.

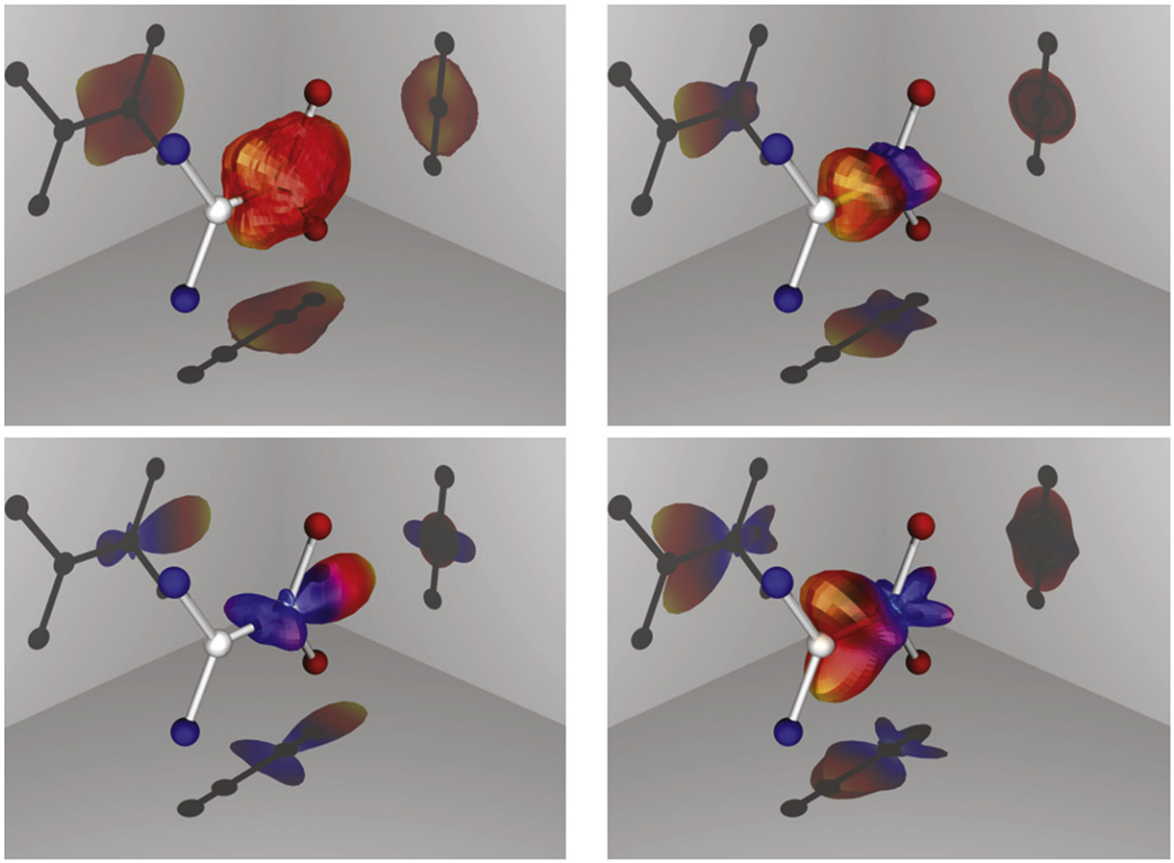

Figure 8. MFPADs of $C_2H_2F_2$ where the carbon on the F_2 side was ionized in experiments performed at two different photon energies: $h\nu = 296$ and $h\nu = 301$ eV. Top row: experiment 0–2 eV and 3–6 eV photoelectrons. Bottom row: complex Kohn results at photoelectron energies of 1.09 and 4.35 eV.

5. Discussion

We have studied the MFPADs for carbon K-edge photoionization of C_2H_6, CF_4 and $C_2H_2F_2$ at photoelectron energies below 10 eV using complex Kohn theoretical calculations and COLTRIMS. The measurements agree rather well overall with the theoretical predictions and remarkably well for the first two molecules. The MFPADs, when integrated over all directions of the photon polarization, yield shapes consistent with the symmetry point group of the target molecule. For C_2H_6, that shape also images the shape of the molecule, with lobes showing preferential ejection along the C–H bonds. For CF_4 a contrasting 'anti-imaging' effect is found, with photoelectrons preferentially ejected in directions between the C–F bonds. A set of measurements and theoretical investigations for $C_2H_2F_2$ was also carried out. As this molecule comprises two energetically non-degenerate carbon K-edges, the emission center of the photoelectron can be chosen in the experiments by considering the photoelectron kinetic energy, yielding distinct differences in the MFPADs. Consistent with what we saw for ethane and carbon tetrafluoride, the MFPADs for $C_2H_2F_2$ shows a combination of both behaviors.

Plesiat *et al* [6] have suggested that the high electronegativity of fluorine creates an excess of negative charge around the fluorine atoms that may repel the escaping photoelectron at lower energies. This classical argument is based essentially on electrostatics. To test this hypothesis, we evaluated the effective electron–ion potentials (static + exchange) for CH_4, CF_4 and $C_2F_2H_2$, using a local model for the exchange interaction (Hara free-electron gas [28]). The static potential is the same numerically generated potential used in the Kohn variational calculations. The equipotential contours for the various cases are plotted in figure 9. A local exchange potential was added to make these figures because there is no way to graphically represent the non-local exchange interaction used in the calculations. It is apparent that those static potentials alone do not provide an obvious basis upon which to conclude that in one case the outgoing photoelectron might avoid a bond axis while in another it might be focused along that axis. In particular, the potentials are everywhere attractive. The electronegativity of the atoms influences the charge density that in turn determines the details of that attractive potential, but it does not produce any barriers. Similar comparisons for LiCCLi and FCCF in an earlier study [29] were more suggestive (the Li-C bond is basically ionic), but a comparison of HCCH and FCCF static potentials in that same study (H–C and F–C bonds are both covalent) was also inconclusive. Although it is tempting to connect the angular distributions with the chemical electronegativity of the atoms involved, we conclude that the behavior of photoelectrons at a few eV cannot be predicted on the basis of simple electrostatics.

The present studies suggest that even though the imaging of molecular geometry by low energy electrons is not a

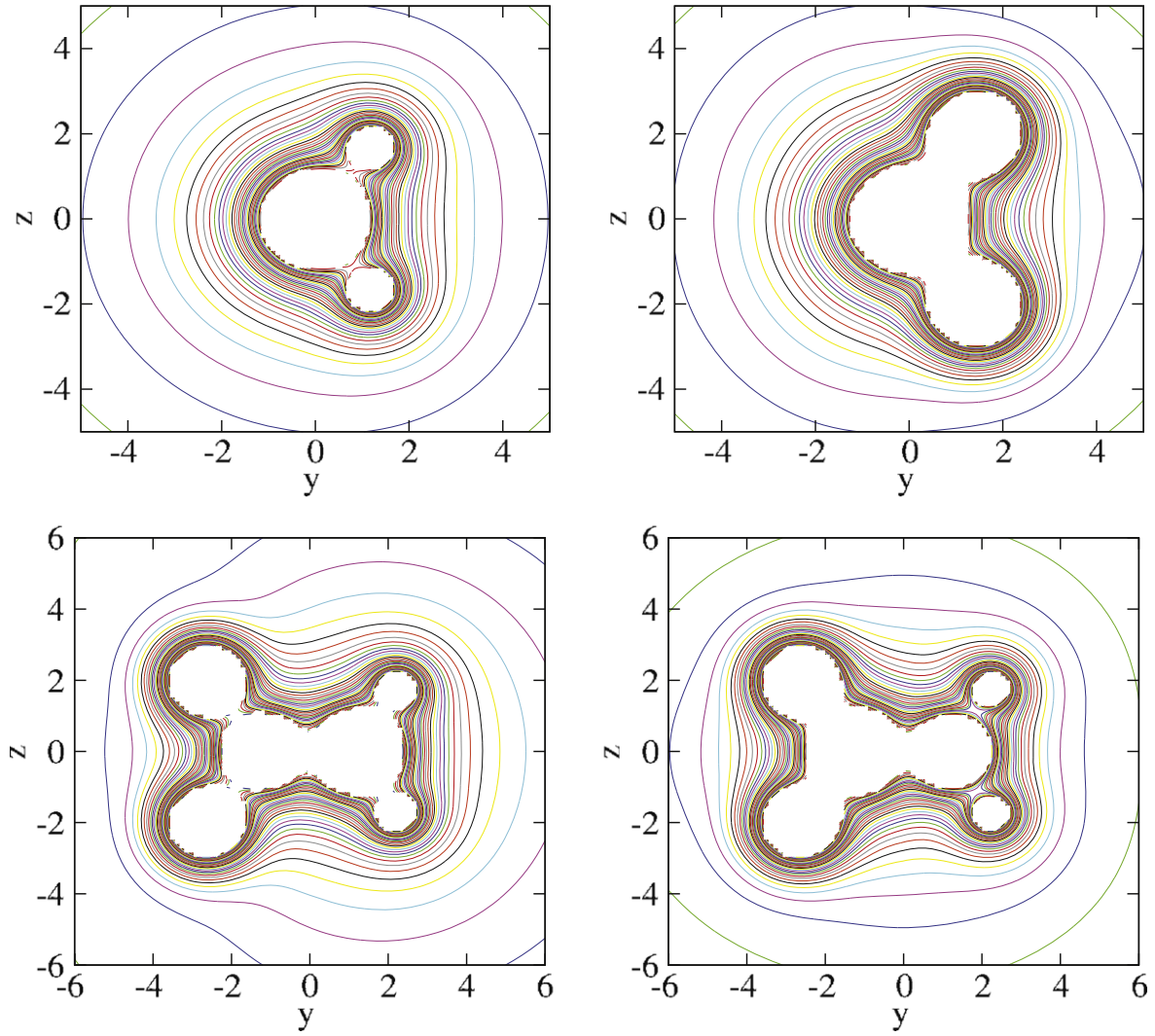

Figure 9. Potential energy functions in the static-exchange approximation with exchange represented by the local Hara free-electron gas approximation. Top left CH_4 in the HCH plane. Top right CF_4 in the FCF plane. Bottom left difluoroethylene in molecular plane with 1s vacancy in C_H. Bottom right difluoroethylene with 1s vacancy in C_F. Contours begin at −2 hartrees in increments of 0.2 hartrees with distances in bohr.

general feature, *ab initio* scattering calculations can aid in the interpretation of measured (polarization averaged) MFPADs and those angular distributions may serve as sensitive indicators of changes in molecular geometry in, for example, time dependent measurements.

Acknowledgments

We acknowledge the financial support of the German Academic Exchange Service (DAAD) and the German Research Foundation (DFG). Work at the University of California, Lawrence Berkeley National Laboratory was performed under the auspices of the US Department of Energy under Contract No. DE-AC02-05CH11231 and was supported by the US DOE Office of Basic Energy Sciences, Division of Chemical Sciences. Work at Auburn University was supported by the US DOE Office of Basic Energy Sciences, Division of Chemical Sciences under grant number DE-FG02-10ER16146. The Kansas State University personnel were supported by grant number DE-FG02-86ER13491 from the same funding agency. One of us (CST) was supported by the US Department of Energy, Office of Science, Office of Workforce Development for Teachers and Scientists (WDTS) under the Visiting Faculty Program (VFP). This research used the Advanced Light Source and resources of the National Energy Research Scientific Computing Center, DOE Office of Science User Facilities supported by the Office of Science of the US Department of Energy under Contract No. DE-AC02-05CH11231. We thank the staff of the Advanced Light Source, in particular beamline 11.0.2 scientists H Bluhm and T Tyliszczak for outstanding support.

References

[1] Arasaki Y, Takatsuka K, Wang K and McKoy V 2010 *J. Chem. Phys.* **132** 124307
[2] Hockett P, Bisgaard C Z, Clarkin O J and Stolow A 2011 *Nat. Phys.* **7** 612

[3] Rescigno T N, Douguet N and Orel A E 2012 *J. Phys. B: At. Mol. Opt. Phys.* **45** 194001
[4] Douguet N, Rescigno T N and Orel A E 2013 *Phys. Rev.* A **88** 013412
[5] Trevisan C S, McCurdy C W and Rescigno T N 2012 *J. Phys. B: At. Mol. Opt. Phys.* **45** 194002
[6] Plésiat E, Decleva P and Martín F 2013 *Phys. Rev.* A **88** 063409
[7] Lucchese R and Stolow A (ed) 2012 *J. Phys. B: At. Mol. Opt. Phys.* **45** 190201
[8] Reid K L 2012 *Mol. Phys.* **110** 131
[9] Williams J B *et al* 2012 *Phys. Rev. Lett.* **108** 233002
[10] Dörner R, Mergel V, Jagutzki O, Spielberger L, Ullrich J, Moshammer R and Schmidt-Böcking H 2000 *Phys. Rep.* **330** 95
[11] Jahnke T, Weber T, Osipov T, Landers A L, Jagutzki O, Schmidt L P H, Cock C L, Prior M K, Schmidt-Böcking H and Dörner R 2004 *J. Electron Spectrosc. Relat. Phenom.* **141** 229
[12] Dowek D, Haouas A, Guillemin R, Elkharrat C, Houver J C, Li W B, Catoire F, Journel L, Simon M and Lucchese R R 2009 *Eur. Phys. J. Spec. Top.* **169** 85
[13] Williams J B *et al* 2012 *J. Phys. B: At. Mol. Opt. Phys.* **45** 194003
[14] Trevisan C, Williams J, Menssen A, Weber T, Rescigno T, McCurdy C W and Landers A 2014 *Bull. Am. Phys. Soc.* **59** K1.0013
[15] Abad L, Bermejo D, Cancio P, Domingo C, Herrero V J, Santos J, Tanarro I and Montero S 1994 *J. Raman Spectrosc.* **25** 589–97
[16] Shimanouchi T 2015 Molecular vibrational frequencies *NIST Chemistry WebBook, NIST Standard Reference Database Number 69* ed P Linstrom and W Mallard (Gaithersburg MD: National Institute of Standards and Technology) p 20899 (http://webbook.nist.gov)
[17] Slater J C 1974 *The Self-Consistent Field for Molecules and Solids: Quantum Theory of Molecules and Solids* vol 4 (New York: McGraw-Hll)
[18] Orel A, Rescigno T N and Lengsfield B H III 1990 *Phys. Rev.* A **2** 5292
[19] Rescigno T N, Lengsfield B H and Orel A E 1993 *J. Chem. Phys.* **99** 5097
[20] Miyabe S, McCurdy C W, Orel A E and Rescigno T N 2009 *Phys. Rev.* A **79** 053401
[21] Haiduke R L A, de Oliveira A E, Moreira N H and Bruns R E 2004 *J. Phys. Chem.* A **108** 866
[22] Okada K *et al* 2005 *J. Electron Spectrosc. Relat. Phenom.* **144–7** 187
[23] Renka R J 1988 *ACM Trans. Math. Softw.* **14** 149
[24] Saito N, Bozek J D and Suzuki I H 1994 *Chem. Phys.* **188** 367
[25] Guillemin R, Stolte W C, Piancastelli M N and Lindle D W 2010 *Phys. Rev.* A **82** 043427
[26] Locht R, Dehareng D and Leyh B 2012 *J. Phys. B: At. Mol. Opt. Phys.* **45** 115101
[27] Landers A L *et al* 2009 *Phys. Rev. Lett.* **102** 223001
[28] Hara S 1967 *J. Phys. Soc. Japan* **22** 710
[29] Fonseca dos Santos S, Douguet N, Orel A E and Rescigno T N 2015 *Phys. Rev.* A **91** 023408